Ilorin Journal of Science
Volume 10, Number 2, 2023, pp. 112 – 128 (Printed in Nigeria)
ISSN: 2408 – 4840 © 2023 Faculty of Physical Sciences, University of Ilorin
https://doi.org/10.54908/iljs.2023.10.02.004

ILORIN JOURNAL OF SCEINCE

ILJS-23-020

Experimental Investigation of Chaos Synchronization Under Different Coupling Schemes

Egunjobi[1*], A I., Ojo[2], K.S., Ajayi[1], K. D., Alabi[1], A. A., Lasisi[1], R. A.

[1]Department of Physics, Federal University of Agriculture, Abeokuta, Ogun state, Nigeria
[2]Department of Physics, University of Lagos, Akoka, Lagos, Nigeria

Abstract

This work presents an experimental implementation of a nonlinear chaotic system using Multisim simulation software and off-the-shelve components. The three-dimensional nonlinear differential equations of Sprott, Rossler, and two-dimensional van der Pol systems were transformed into an electronic circuit. We derived the differential equations for the systems using Kirchoff's Laws. An Op-amp is used as an integrator and inverter in the circuits while a multiplier is used for deriving the nonlinear terms in the systems. The transformation of the system from periodic to chaotic oscillation was observed. Two identical systems were coupled using bidirectional and cyclic coupling schemes, synchronization, and the advantages of cyclic coupling configuration over the convectional bidirectional schemes of the new systems are reported.

Keywords: Cyclic Coupling, Diffusive Coupling, Synchronization, Coupling Strength and Electronics Implementation

1. Introduction

Experimental investigation of chaos synchronization involves practically implementing and observing chaotic systems under different coupling schemes. The key steps in such an investigation include System Selection, Coupling Implementation, Data Collection, and Analysis. Since the discovery of chaos by Lorenz to describe the simplified Rayleigh–Benard problem, unpredictable dynamical behaviour has been found in many other natural and artificial systems and has great potential usage in technological development, such as in communication systems, philosophy and complexity science, psychology and neuroscience, information security, engineering and control systems, finance and economics, biological systems, weather forecasting, and climate science (Somayeh *et al.*, 2020; Alexey, 2023; Bowen and Lingfeng, 2023; Li *et al.*, 2023; Sundarapandian *et al.*, 2018).

The use of different coupling schemes to achieve synchronization and stability criteria in dynamic systems has been of great interest to researchers for the past two decades. The

Corresponding Author: **Egunjobi, A. I.**

Email**:** egunjobiai@funaab.edu.ng

unidirectional and bidirectional linear couplings were mainly explored in two or many oscillators (Yeldesbay *et al.*, 2014). Synchronization in two or more dynamical systems occurs when the chaotic systems, driven by similar dynamics, achieve a correlated behaviour. In an unpredictable system, adjustment of initial conditions leads to vastly different changes in the system dynamics as time changes (Massimo *et al.,* 2010).

The trajectories of chaotic systems can become identical under certain conditions, such as: identical dynamics, coupling strength, coupling mechanism, and so on. The general idea of this phenomenon is to exploit the inherent unpredictability and sensitivity to initial conditions in chaotic systems for secure communication, data encryption (Alvarez and Li, 2006), Secure Key Distribution (Atsushi *et al.,* 2008), Neural Networks and Chaos Synchronization (Pathak *et al.,* 2018), Biomedical Signal Processing (Marwan *et al.,* 2007), Optical Communication (Larger *et al.,* 2015).

Chua, 1983 implemented a simple electronic circuit that exhibited chaotic behaviour, it is the earliest circuit experiment of chaotic systems, and it played a vital role in demonstrating the feasibility of chaos in physical systems (Chua, 2006). The electronic coupling of chaos systems has been important to understanding some basic applications of chaos. For unidirectional coupling, commonly called master-slave coupling, the systems are connected through the resistor and a unity-gain operational amplifier (OP Amp) (Larger *et al.,* 2015).

On the other hand, for master-master or slave-slave coupling, also referred to as bidirectional or diffusive coupling, the systems are coupled through the same variables, this can be found mostly in many natural systems (Pikovsky *et al.,* 2001), for example, in gap junction of neurons (Skinner *et al.,* 1999). The coupling is realized by joining the same points of indistinguishable circuits through a resistor, it leads to reciprocal interaction between the two systems then synchronization takes place. The major task in the study of synchronization in chaotic systems is determining the critical coupling for which a synchronized system is stable. The coupling configuration and topology are vital in achieving synchronization stability (Christophe *et al.,* 2010).

Motivated by the numerous applications of chaotic systems, we reported the experimental investigation of bidirectional and cyclic coupling on the synchronization of identical chaotic systems such as autonomous Rössler and Sprott systems, and non-autonomous van der Pol systems, to develop a clear understanding of the principles of chaos synchronization, to explore various coupling schemes and analyze how these different schemes affect the synchronization of chaotic systems. In Sect. 2, we describe the coupling methods adopted. Sect. 3, systems implementation. In sect. 4, bidirectional and cyclic coupling implementation. Finally, section 5, provides the conclusion of this work.

2. Description of the Method

2.1. Bidirectional Coupling:

$$\dot{x}_1 = -x_2 - x_3$$
$$\dot{x}_2 = x_1 + bx_2 \qquad (1)$$
$$\dot{x}_3 = c + x_3(x_1 - d),$$

where *b, c, and d* are system parameters with the following values b = c = 0.2 and d = 5.7 for chaotic behaviour. Equation (1) represents the Rossler system chosen to elaborate on bidirectional coupling. Oscillators 1 & 2 are the first and second systems coupled bi-directionally into each other.

Oscillator-1:

$$\dot{y}_1 = -y_2 - y_3 + U_{y_1}$$
$$\dot{y}_2 = y_1 + by_2 + U_{y_2} \qquad (2)$$
$$\dot{y}_3 = c + y_3(y_1 - d) + U_{y_3},$$

Oscillator-2:

$$z_1 = -z_2 - z_3 + U_{z_1}$$
$$\dot{z}_2 = z_1 + bz_2 + U_{z_2} \qquad (3)$$
$$\dot{z}_3 = c + z_3(z_1 - d) + U_{z_3},$$

where $U_y = [U_{y_1}\ U_{y_2}\ U_{y_3}]^T$ and $U_z = [U_{z_1}\ U_{z_2}\ U_{z_3}]^T$ are the system controllers. The controllers are added to equations 1 and 2 to set up the mutual interactions between the two systems. The error function is defined by equation (4)

$$e(t) = \beta y - \alpha x, \qquad (4)$$

where β and α are constant.

2.2. Cyclic coupling

Cyclic coupling is similar to mutual coupling. It is a situation whereby an oscillator is coupled to another oscillator via a particular state variable and the first system receives a feedback signal from the second oscillator through another state variable leading to mutual interaction between the systems (Olusola *et al.*, 2013), the phenomenon is illustrated in Figure 1.

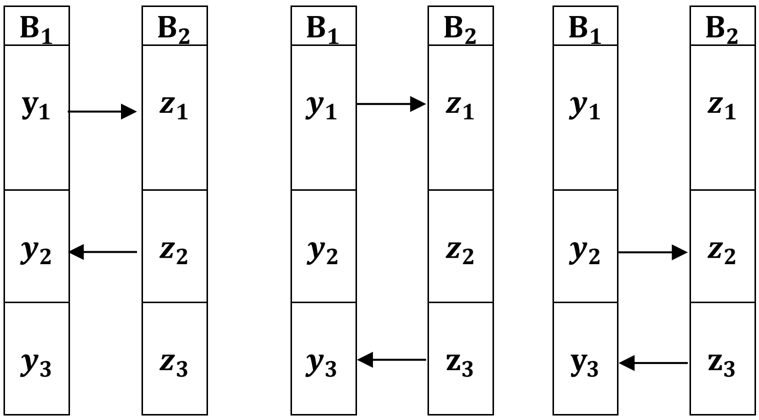

Figure 1: Schematics of two identical systems (B_1 and B_2) interacting via cyclic coupling with different topologies.

There are six topologies of cyclic coupling possible for 3D systems, three are independent while the other three are symmetric for identical oscillators. Considering two pairs of variables, the three independent options are (i) $y_1 \rightarrow z_1$, $y_2 \leftarrow z_2$, (ii) $y_1 \rightarrow z_1$, $y_3 \leftarrow z_3$, and (iii) $y_2 \rightarrow z_2$, $y_3 \leftarrow z_3$ as illustrated in Figure 1. Using Equation (1), we present an example of two identical cyclic coupled Rossler systems in equations (5 and 6).

Oscillator-A:

$$\begin{aligned} \dot{y}_1 &= -y_2 - y_3 \\ \dot{y}_2 &= y_1 + by_2 + k\,(z_2 - y_2) \\ \dot{y}_3 &= c + y_3(y_1 - d). \end{aligned} \tag{5}$$

Oscillator-B:

$$\begin{aligned} z_1 &= -z_2 - z_3 + k\,(y_1 - z_1) \\ \dot{z}_2 &= z_1 + bz_2 \\ \dot{z}_3 &= c + z_3(z_1 - d). \end{aligned} \tag{6}$$

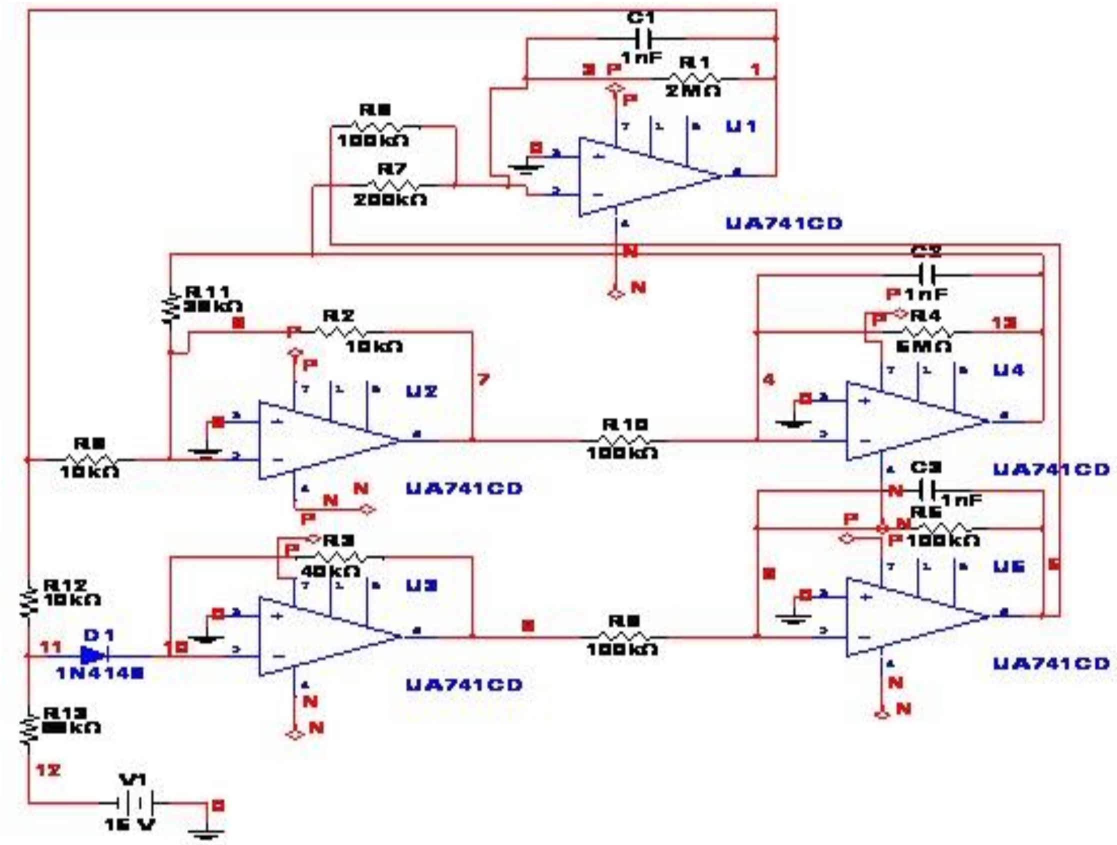

Figure 2: Schematic diagram of Rossler circuit (Ranjib *et al*., 2012).

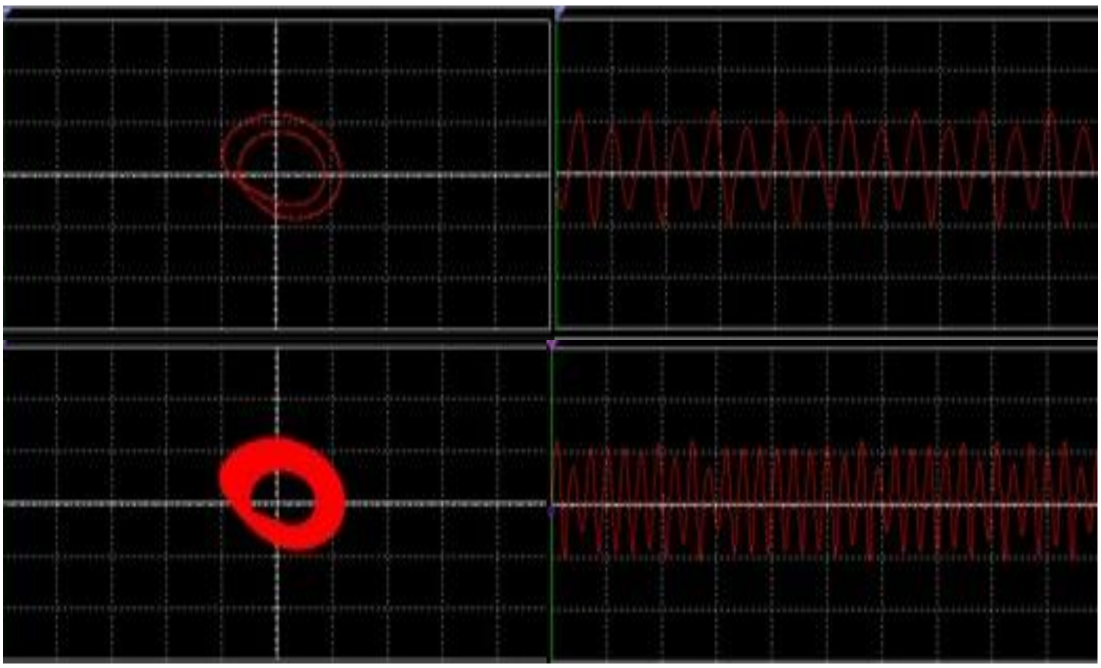

Figure 3: MultiSim oscilloscope pictures of Rossler oscillator showing transits from periodic to chaotic signal, 2D projection of the attractors on the left panel and time series on the right panel for period two R11 = 41.5 kΩ, and for chaotic signal 0 <R11≤35.1 kΩ.

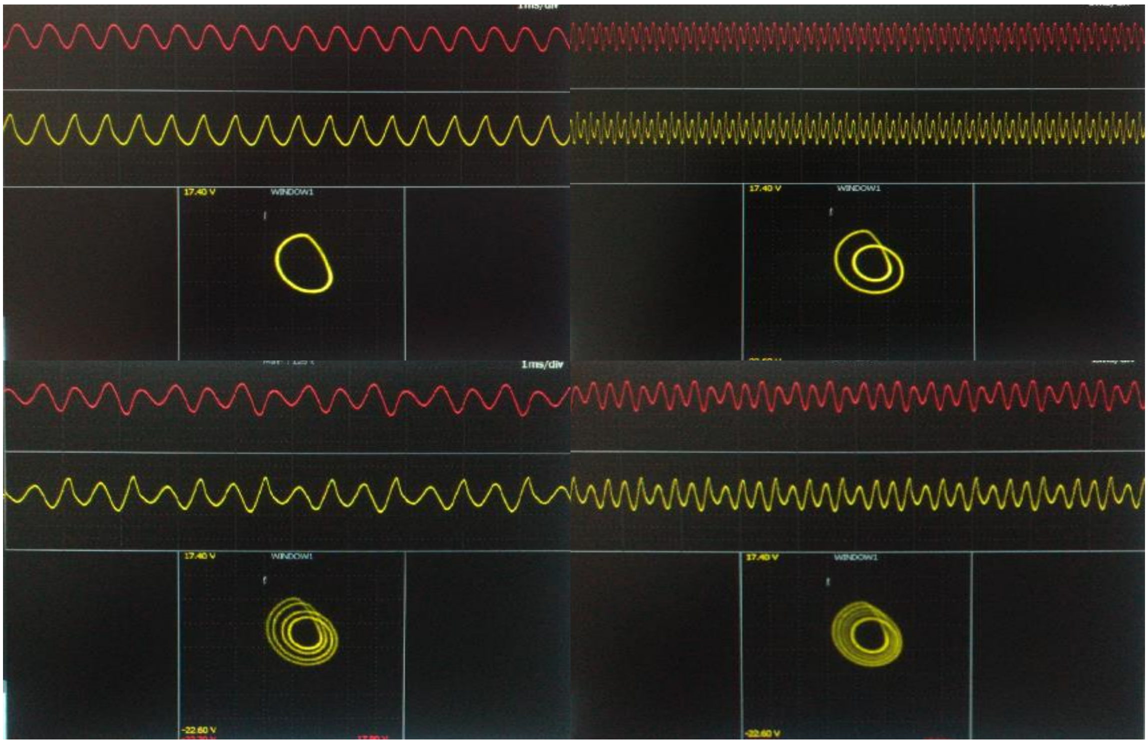

Figure 4: Experimental oscilloscope pictures of the Rossler oscillator showing transits from periodic to chaotic signals. The first row shows oscillation for periods one and two for R11 = 62.1 kΩ and R11 = 55.0 kΩ. The second row shows oscillations for period four and chaotic signal at R11 = 46.7 kΩ and $0 < R11 \leq 41.2$ kΩ respectively.

3. Systems Implementation

Figure 2 represents the circuit diagram for the Rossler oscillator. The circuit consists of resistors R1 – R13, capacitors C1 – C3, potentiometer, Op-amps UA741CD (U1 - U5) powered by ± 12 V, and voltage supply V1 which represents parameter c. The circuit was built using MultiSim simulation software and in the laboratory using off-the-shelf components on the breadboard. The 741 serves as an integrator and inverter for the input signals. The following relation relates the variable resistor R11 in Figure 2 to the parameter b in equation (1); $b = {}^{R}/_{R11}$, where the value of R = 10 Ω. Figure 3 shows the MultiSim pictures of the system as it transits from periodic and chaotic attractors as the plot of x vs y takes the output from U1 and U4.

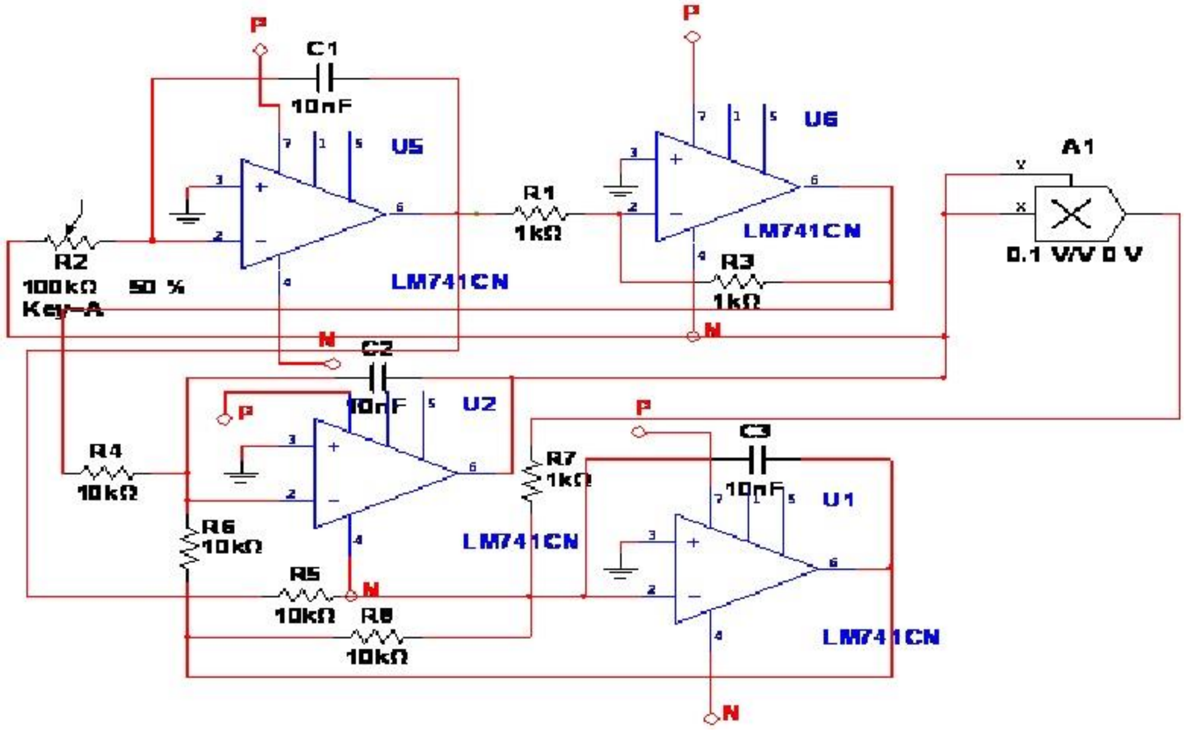

Figure 5: Schematic diagram of Sprott circuit (Ioan *et al.*, 2008; Sprott 1994).

The experimental results shown in Figure 4 are found to be in good agreement with the computer simulation results as the attractor was observed to change from periodic to chaotic signal as the value of R11 reduces from 60.1 kΩ to 41.2 kΩ. Following the same procedure, the dynamic behaviours of Sprott and van der Pol systems were also studied, the time series and the corresponding phase portrait are depicted in Figures (5 –10). The MultiSim and experimental results are in agreement with each other.

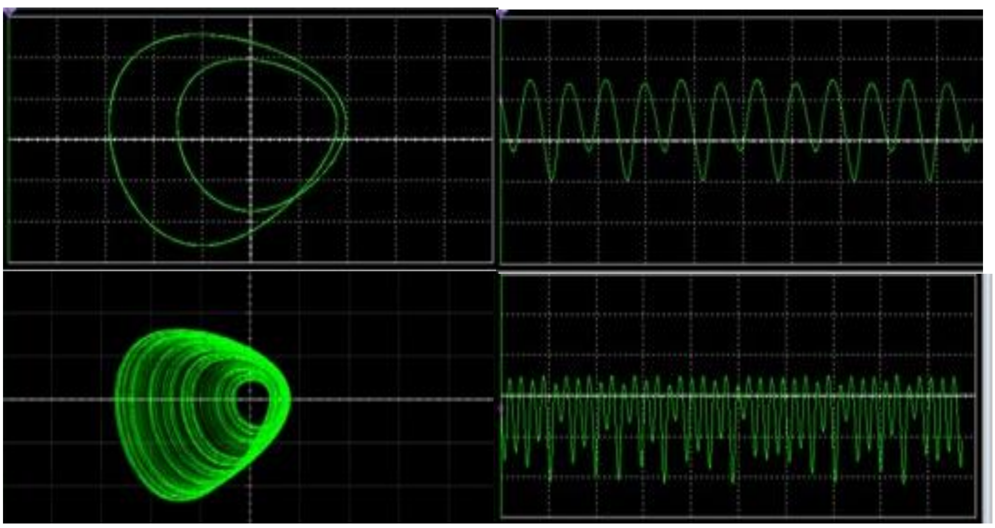

Figure 6: MultiSim oscilloscope pictures of Sprott oscillator showing transits from periodic to chaotic signal, 2D projection of the attractors on the left panel, and time series on the right panel. For period two R11 = 55.0 kΩ, and chaotic signal R11≤ 41.2 kΩ.

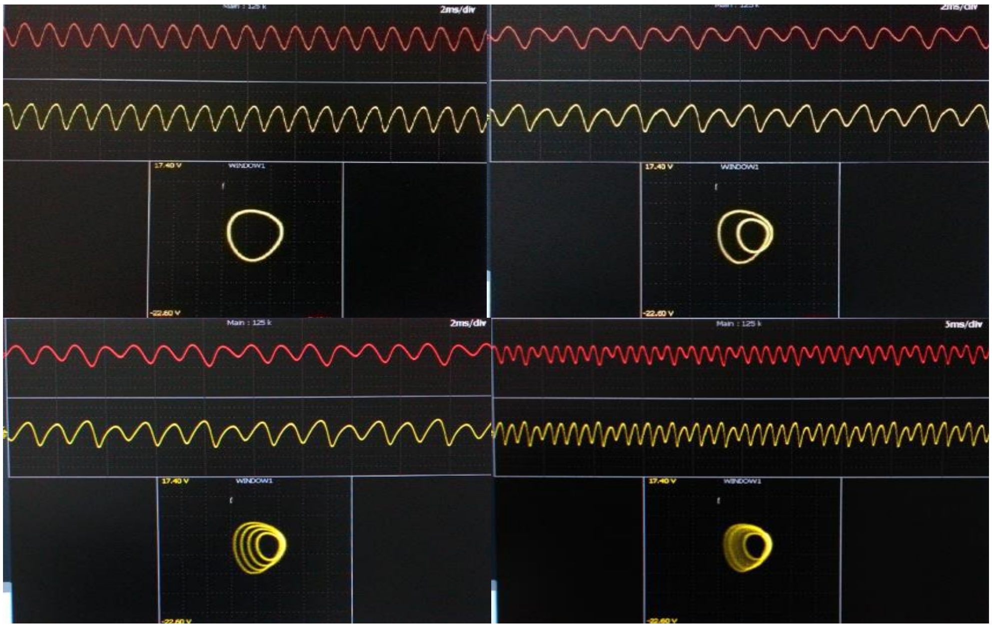

Figure 7: Experimental oscilloscope pictures of Sprott oscillator showing transits from periodic to chaotic signal. The first row shows oscillation for periods one and two for R2 = 71.5 kΩ and R2 = 69.9 kΩ. The second row shows oscillation for period four and chaotic signal at R11 = 66.9 kΩ and 0 <R11 ≤ 61.9 kΩ respectively.

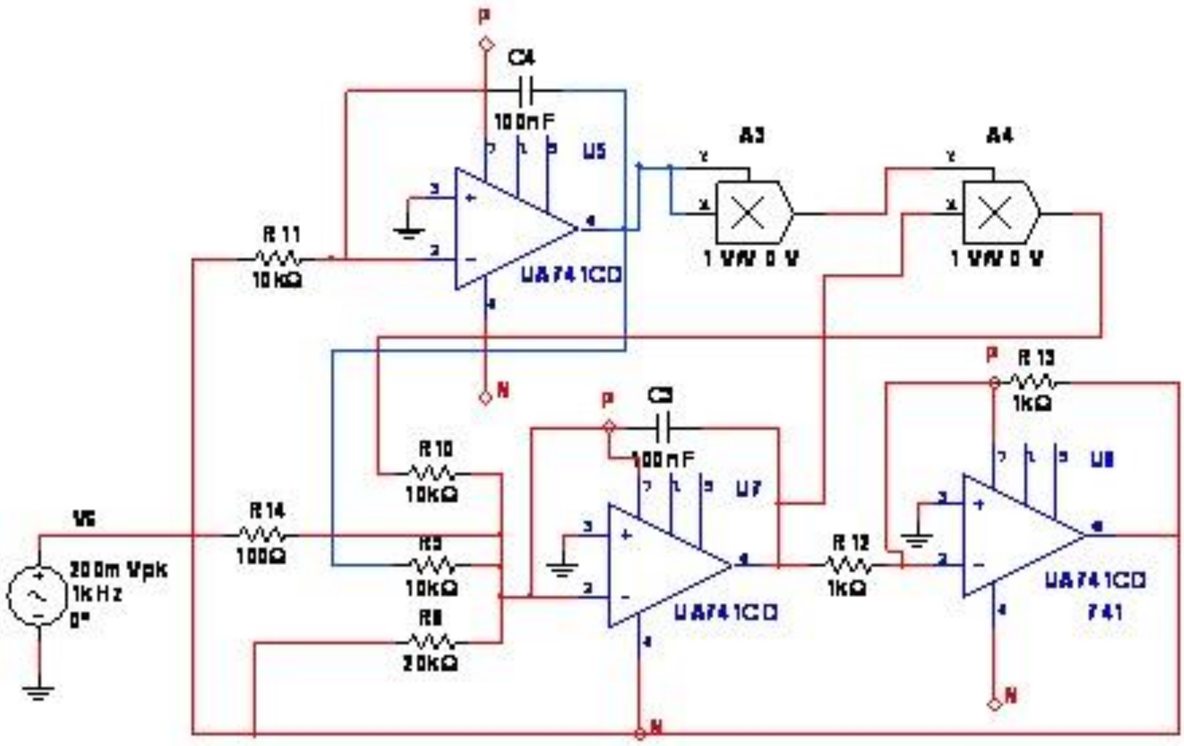

Figure 8: Schematic diagram of van der Pol circuit (Makouo and Woafo, 2017; Sourav *et al.*, 2011)

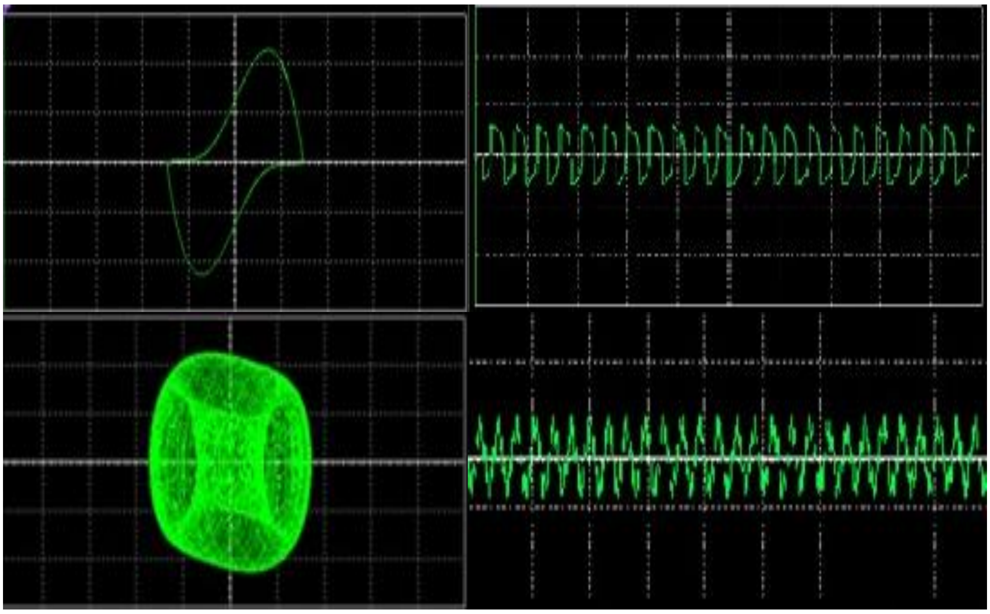

Figure 9: MultiSim oscilloscope pictures of van der Pol oscillator showing transits from periodic to chaotic signal, 2D projection of the attractors on the left panel, and time series on the right panel. For the limit cycle, R8 is 74.4 kΩ, and for the chaotic signal 0 <R8 ≤ 49 kΩ.

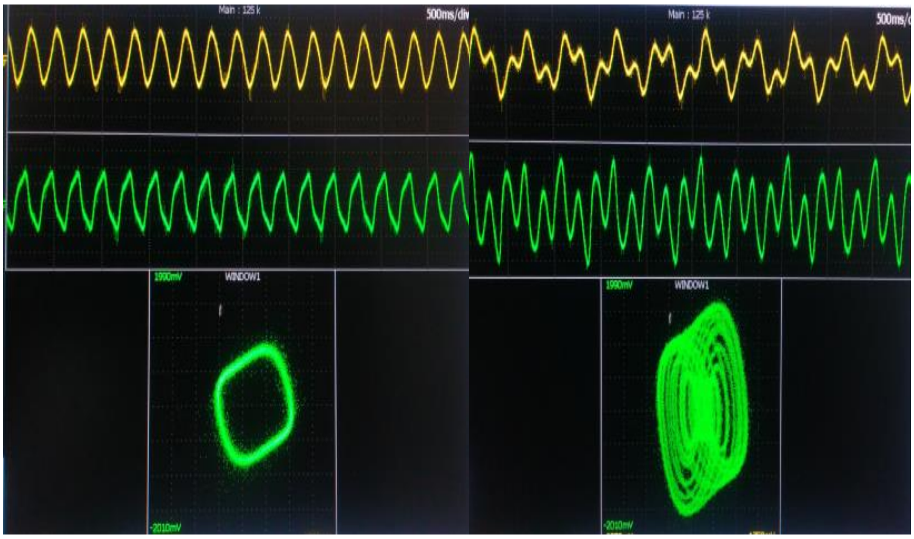

Figure 10: Experimental oscilloscope pictures of van der Pol oscillator showing transits from limit cycle to chaotic signal. The first two rows show the time series and the third row shows the attractors. For the limit cycle, R8 is 67.4 kΩ, and for the chaotic signal 0 <R8 ≤ 47.7 kΩ.

4. Bidirectional and Cyclic Coupling Implementation

Our purpose is to describe how we use electronic circuits to implement bidirectional and cyclic coupling of two identical autonomous and non-autonomous systems. This was carried out using MultiSim simulation software and off-the-shelve components. Figures (11 and 12) show the coupling forms using the Sprott system as a case study, R2 and R10 represent the potentiometer for each of the oscillators (B_1 and B_2) and have fixed values for the systems to be identical. k_1 and k_2, which are functions of R17 and R18, represent the coupling strength of the system. The oscillators were constructed independently and tested to confirm chaotic dynamics. In other to achieve 'identical' systems, the same type of electronic components was used in both circuits. The first oscillator B_1 uses four integrators (U1, U2, U5, and U6) to simulate the output voltages, and a multiplier A_1 to simulate the square nonlinearity in the system. In contrast, the second oscillator B_2 uses integrator (U3, U4, U7, and U8) with multiplier A_2.

Table 1: Threshold couplings based on MultiSim simulation for mutual coupling and cyclic coupling indifferent circuits

	Diffusive coupling		
	$y_1 \leftrightarrow z_1$	$y_2 \leftrightarrow z_2$	$y_3 \leftrightarrow z_3$
Sprott	$0 < R_c \leq 123.50$ kΩ	$0 < R_c \leq 197$ kΩ	No CS
Rossler	$3.08k < R_c \leq 50$ kΩ	$0 < R_c \leq 67$ kΩ	No CS
van der Pol	$0 < R_c \leq 220$ kΩ	$0 < R_c \leq 152$ kΩ	
	Cyclic coupling		
	$y_1 \rightarrow z_1$, $y_2 \leftarrow z_2$	$y_1 \rightarrow z_1$, $y_3 \leftarrow z_3$	$y_2 \rightarrow z_2$, $y_3 \leftarrow z_3$
Sprott	$0 < R_c \leq 249.70$ kΩ	$0 < R_c \leq 56.20$ kΩ	$0 < R_c \leq 49.50$ kΩ
Rossler	$0 < R_c \leq 84.50$ kΩ	$1.21k < R_c \leq 41.3$ kΩ	$1.21k < R_c \leq 48.50$ kΩ
van der Pol	$0 < R_c \leq 122.7$ kΩ		

Table 2: Threshold couplings based on experiments for mutual coupling and cyclic coupling in different circuits

	Diffusive Coupling		
	$y_1 \leftrightarrow z_1$	$y_2 \leftrightarrow z_2$	$y_3 \leftrightarrow z_3$
Sprott	$0 < R_c \leq 125$ kΩ	$0 < R_c \leq 200$ kΩ	No CS
Rossler	$4.10 < R_c \leq 55$ kΩ	$0 < R_c \leq 66.67$ kΩ	No CS
van der Pol	$0 < R_c \leq 229$ kΩ	$0 < R_c \leq 157$ kΩ	
	Cyclic Coupling		
	$y_1 \rightarrow z_1$, $y_2 \leftarrow z_2$	$y_1 \rightarrow z_1$, $y_3 \leftarrow z_3$	$y_2 \rightarrow z_2$, $y_3 \leftarrow z_3$
Sprott	$0 < R_c \leq 251$ kΩ	$0 < R_c \leq 58.82$ kΩ	$0 < R_c \leq 50$kΩ
Rossler	$0 < R_c \leq 84.50$ kΩ	$1.21k < R_c \leq 41.3$ kΩ	$1.21k < R_c \leq 48.50$ kΩ
Van der Pol	$0 < R_c \leq 125$ kΩ		

Figures (13 and 14) show that complete synchronization (CS) (left panel) occurred only on ($x_1 \leftrightarrow y_1$) and ($x_2 \leftrightarrow y_2$). The results in Figures (15 and 16) obtained for the cyclic coupling formation show that CS occurred on ($x_1 \leftrightarrow y_1$), ($x_2 \leftrightarrow y_2$) and ($x_3 \leftrightarrow y_3$). This implies that the coupled nonlinear oscillators evolve in CS when the conventional bidirectional coupling fails to produce synchronous behaviour. Tables 1 and 2 summarize the result obtained for threshold couplings for the three systems considered using the two methods adopted. Complete synchronization occurred at different coupling strengths as shown in the Tables. The simulation and experiment results show that the systems synchronize well. We presented the experimental setup for coupled and uncoupled systems in Figure 17.

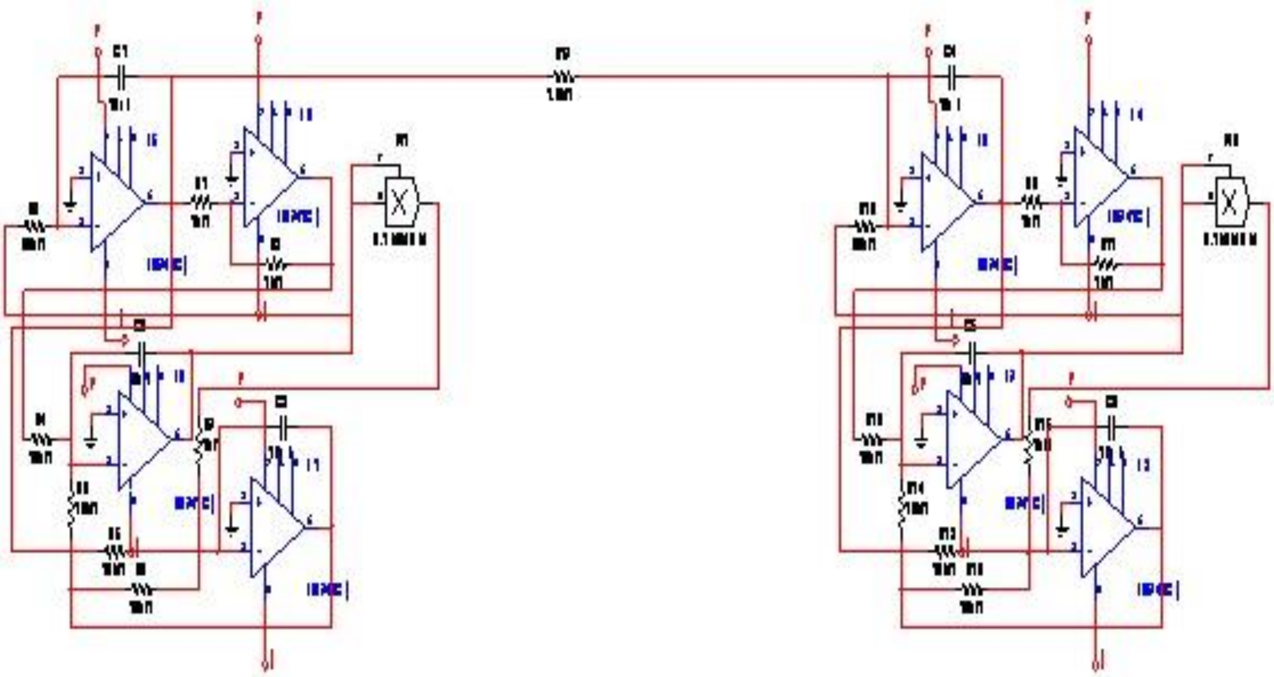

Figure 11: Schematic diagram of bidirectional coupled Sprott System

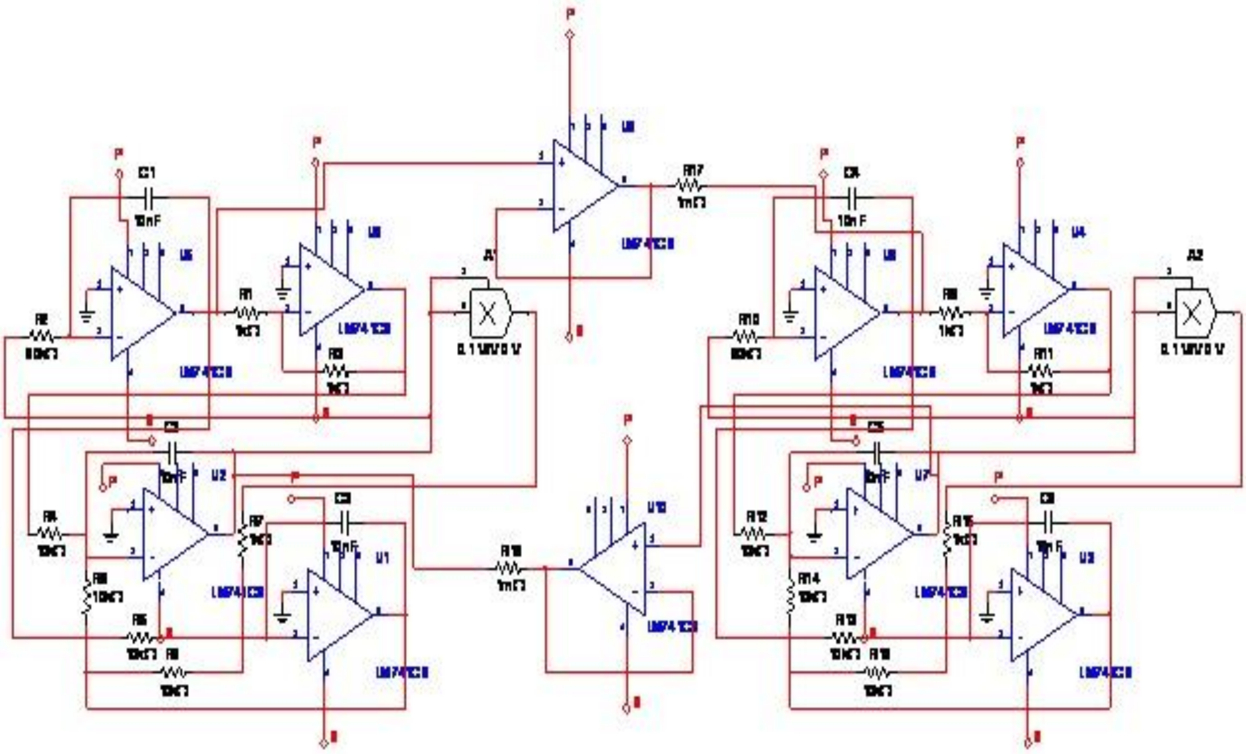

Figure 12: Schematic diagram of cyclic coupled Sprott System

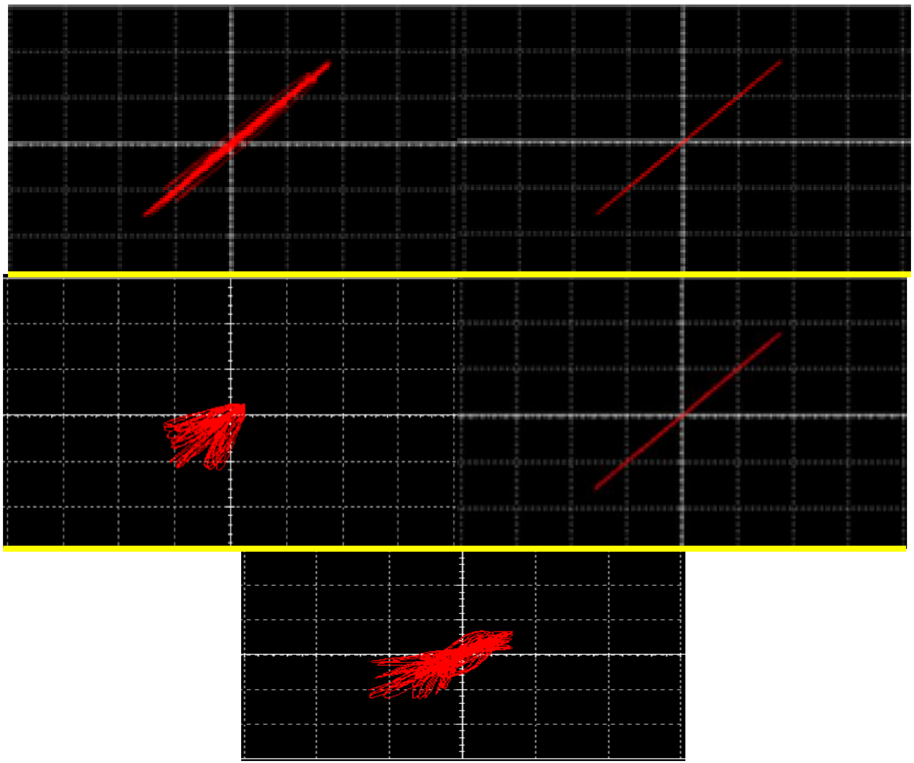

Figure 13: MultiSim oscilloscope pictures of mutually coupled Sprott oscillator. The left side shows no CS and the right side shows CS. First row ($y_1 \leftrightarrow z_1$) CS occurred at $0 < R_c \leq 123.50$ kΩ, second row ($y_2 \leftrightarrow z_2$) CS occurred at $0 < R_c \leq 197$ kΩ, and third row ($y_3 \leftrightarrow z_3$) no CS.

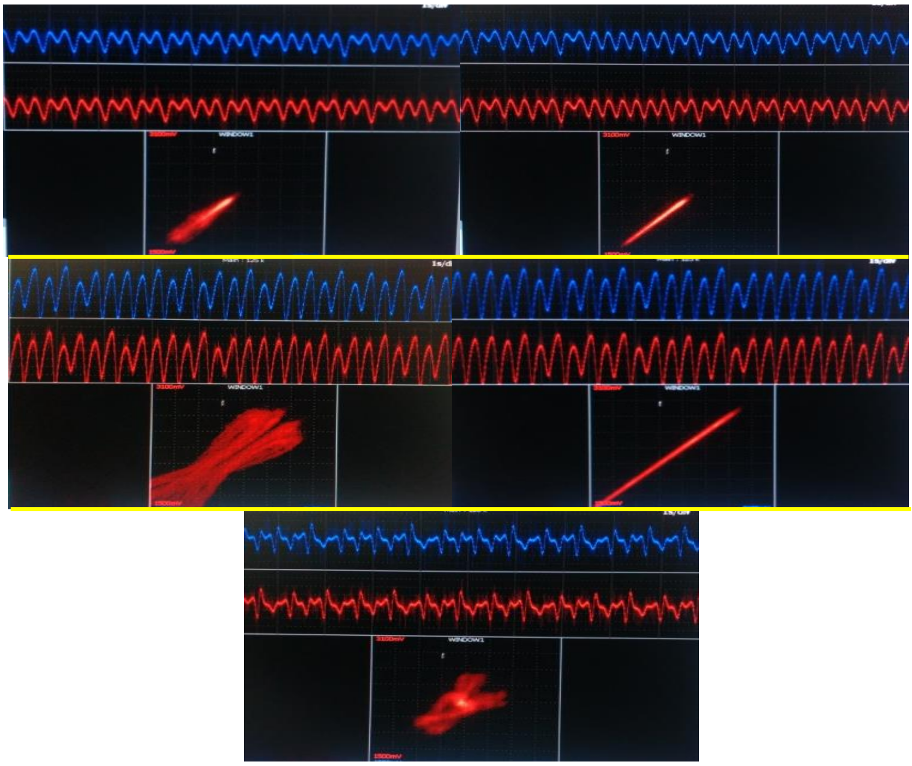

Figure 14: Experiment with oscilloscope pictures of a mutually coupled Sprott oscillator. The left side shows no CS and the right side shows CS. First row ($y_1 \leftrightarrow z_1$) CS occurred at $0 < R_c \leq 125$ kΩ, second row ($y_2 \leftrightarrow z_2$) CS occurred at $0 < R_c \leq 200$ kΩ, and third row ($y_3 \leftrightarrow z_3$) no CS.

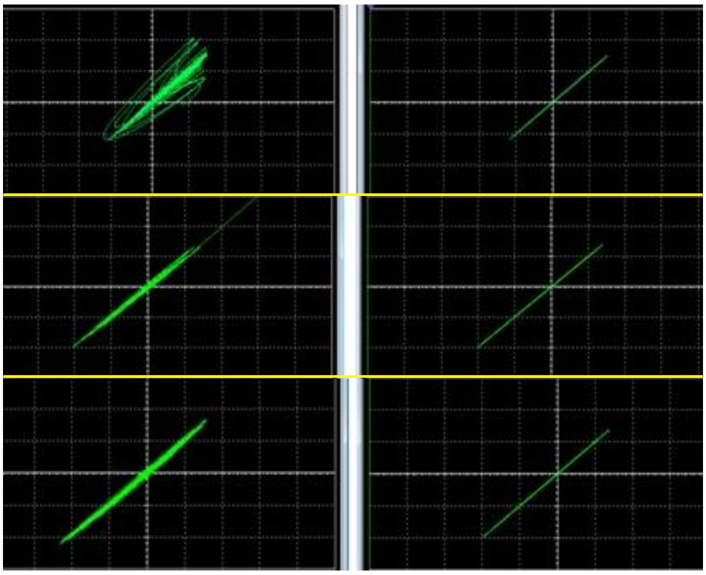

Figure 15: MultiSim oscilloscope pictures of cyclic coupled Sprott oscillator. The left panel shows no complete synchrony (CS) and the right panel shows CS. First row ($y_1 \rightarrow z_1$, $y_2 \leftarrow z_2$) CS occurred at $0 < R_c \leq 249.70$ kΩ, second row ($y_1 \rightarrow z_1$, $y_3 \leftarrow z_3$) CS occurred at $0 < R_c \leq 56.20$ kΩ, and third row ($y_2 \rightarrow z_2$, $y_3 \leftarrow z_3$) CS occurred at $0 < R_c \leq 49.50$ kΩ.

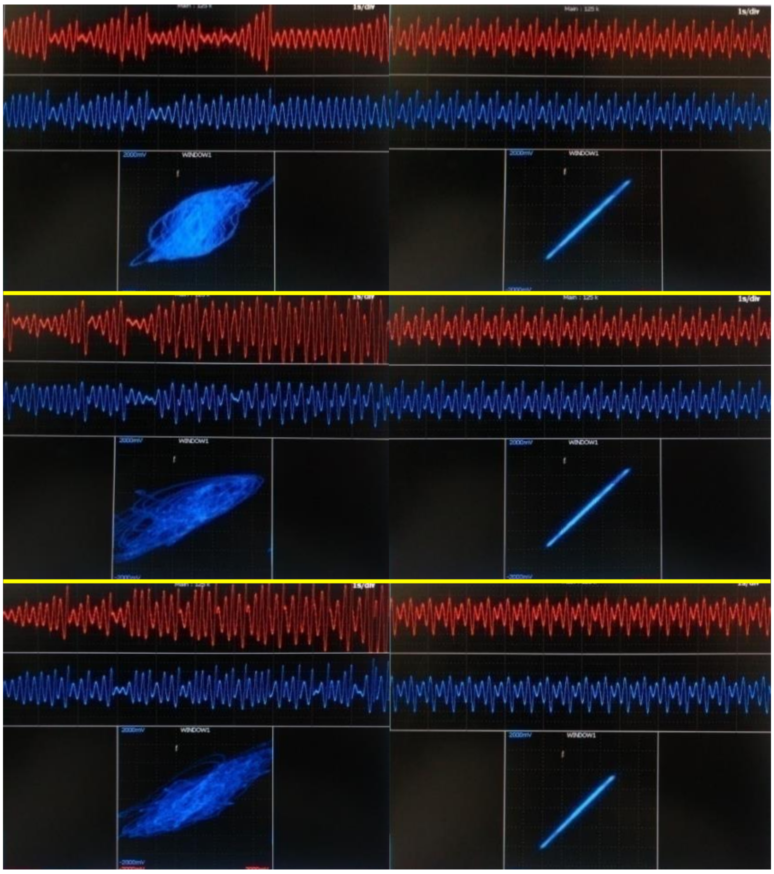

Figure 16: Experiment oscilloscope pictures of cyclic coupled Sprott oscillator. The left panel shows no complete synchrony (CS) and the right panel shows CS. First row ($y_1 \rightarrow z_1$, $y_2 \leftarrow z_2$) CS occurred at $0 < R_c \leq 251$ kΩ, second row ($y_1 \rightarrow z_1$, $y_3 \leftarrow z_3$) CS occurred at $0 < R_c \leq 58.82$ kΩ, and third row ($y_2 \rightarrow z_2$, $y_3 \leftarrow z_3$) CS occurred at $0 < R_c \leq 50$ kΩ.

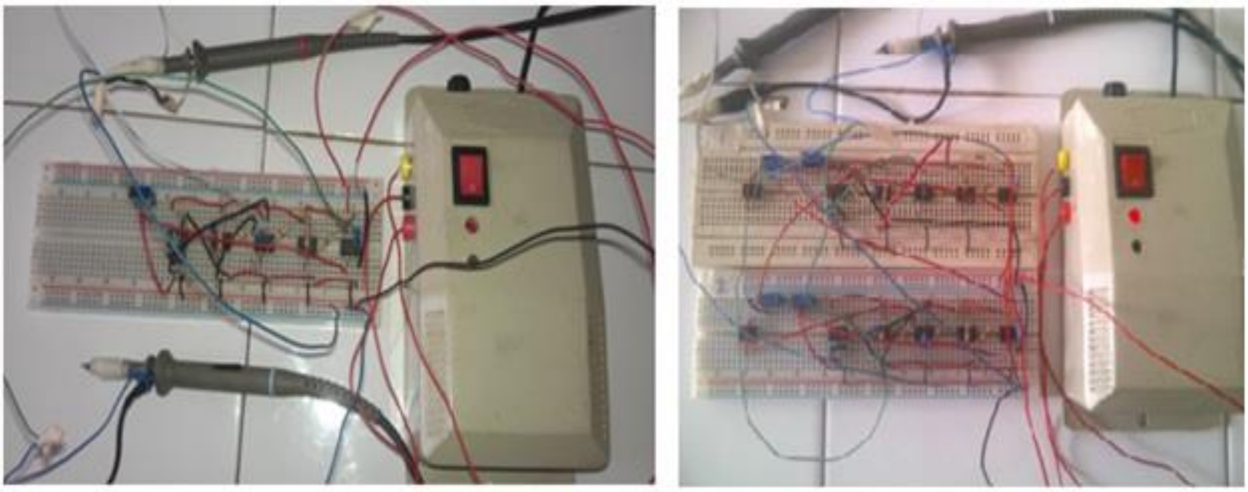

Figure 17: Experiment setup for uncoupled and coupled Sprott systems

5. Conclusions

Experimental investigation of chaos synchronization under different coupling schemes is a rich and evolving field. It combines theoretical insights with practical experimentation, offering deep understanding and innovative applications in science and engineering. Its applications include **Secure Communications, Neuroscience, Biology, and so on.** The choice of coupling scheme and system, along with rigorous experimental methodology, are critical for uncovering the nuanced behaviour of synchronized chaotic systems. In summary, the exciting and interesting dynamical behaviour of the autonomous Sprott oscillator, Rossler oscillator, and non-autonomous forced van der Pol oscillator have been studied.

The system dynamics as it transits from periodic to chaotic motion have been established numerically using MultiSim electronic simulation software and experimentally using off-the-shelve electronic components. Components used for implementation include operational amplifiers, multipliers, resistors, capacitors, diodes, and Arduino UNO microcontroller among others. The system models differential equations were integrated using Op-amp 741; this Op-amp was also used for inverting input signals. For simplicity, the designed circuits were first implemented on MultiSim 12.0 circuit design software.

The possibility of synchronizing two identical systems via bidirectional and cyclic coupling using off-the-shelve components is a subject of interest and can be useful for scientific and engineering purposes. Synchronization behaviour of identical nonlinear oscillators such as Sprott, Rossler, and van der Pol have been studied using diffusive coupling and cyclic coupling. First, the numerical determination of threshold coupling was carried out using MultiSim software. The numerical results were confirmed through experimental study via the use of off-the-shelve electronic components on the breadboard and it was found that both approaches were in good agreement. Furthermore, it was established that applying cyclic coupling on some variables led coupled nonlinear oscillators to evolve into CS where the conventional bidirectional coupling was unable to produce synchronous behaviour. Thus, we propose that a cyclic coupling configuration may be a good replacement for the conventional diffusive coupling formation in the study of synchronization behaviour in coupled nonlinear oscillators.

References

Alexey, T., (2023). A case for chaos theory inclusion in neuropsychoanalytic modeling. *An Interdisciplinary Journal for Psychoanalysis and the Neurosciences*, **25(1)**, 43-52.

Alvarez, G., and Li, S. (2006). Some basic cryptographic requirements for chaos-based cryptosystems. *International Journal of Bifurcation and Chaos*, **16**(8), 2129-2151.

Atsushi, U., Kazuya, A., Masaki, I., Kunihito, H., Sunao, N., Hiroyuki, S., Isao, O., Takayuki, K., Masaru, S., Shigeru, Y., Kazuyuki, Y., and Peter, D. (2008). Fast physical random bit generation with chaotic semiconductor lasers. *Nature Photonics*, **2**(12), 728-732.

Bowen, Z., and Lingfeng, L. (2023). Chaos-Based Image Encryption: Review. *Application, and Challenges. Mathematics*, **11**(11): 2585

Christophe, L., and Luis, A. (2010). The interplay. *Phys. Rev*. E **82**, 016204.

Chua, L.O. (1983). Nonlinear circuits and systems. *IEEE Press*

Chua, L.O. (2006). The genesis of Chua's circuit. *International Journal of Bifurcation and Chaos*, **16(**6), 1649-1664.

Ioan, G., Padmanaban, E., Prodyot, K.R., and Syamal K.D. (2008). Designing Coupling for Synchronization and Amplification of Chaos. *Physical Review Letters*, 0031-9007/08/100(23)/234102(4).

Larger, L., Soriano, M. C., Brunner, D., Appeltant, L., Gutierrez, J. M., Pesquera, L., Mirasso, C. R., and Fischer, I. (2015). Photonic information processing beyond Turing: an optoelectronic implementation of reservoir computing. *Optics Express*, **23**(3), 1470-1491.

Li, Y., Zhan, L., and Xinghu Y. (2023). Adaptive model predictive control based on neural networks for Hover attitude tracking with input saturation and unknown disturbances. *Sage Journals*, **46**(3), 524-537.

Makouo, L., Woafo, P. (2017). Experimental observation of bursting patterns in Van der Pol oscillators. *Chaos, Solitons and Fractals*, **94**, 95–101.

Marwan, N., Carmen R.M., Marco T., Jürgen K. (2007). Recurrence plots for the analysis of complex systems. *Physics Reports*, **438(**5–6), 237- 329.

Massimo, C., Fabio, C., Vulpiani, A. (2010). Chaos: From Simple Models to Complex Systems. *World Scientific: Singapore*, 17, 1 – 480.

Olusola, O.I., Njah, A.N., and Dana, S. K. (2013). Synchronization in chaotic oscillators by cyclic coupling. *Eur. Phys. J. Special Topics*, **222**, 927–937.

Pathak, J, Zhixin L, Brian R. H, G., Edward O. (2018). Using machine learning to replicate chaotic attractors and calculate Lyapunov exponents from data. Chaos: *An Interdisciplinary Journal of Nonlinear Science*, **28(4)**, 041102.

Pikovsky, A. S, Rosenblum, M. G, and Kurths, J. (2001). Synchronization: A Universal Concept in Nonlinear Science. *Cambridge University Press, Cambridge, England*.

Ranjib B., Dibakar G., Padmanaban, E., Ramaswamy R., Pecora M.L., and Syamal K.D. (2012). Enhancing synchrony in chaotic oscillators by dynamic relaying. *Physical Review E* **85,** 027201.

Skinner, F. K, Zhang, L, Perez Velazquez, J. L, Carlen, P. L, Neurophysiol J. (1999). Dynamical Systems in Neuroscience: The Geometry of Excitability and Bursting. *MIT, Cambridge, MA*, **81**(3), 1274.

Somayeh H., Mohammad A.P., Saleh M., and Mahdi R.A. (2020). Design a secure communication system between the base transmitter station and mobile equipment based on finite-time chaos synchronization. *International Journal of Systems Science*, **51**(2), 1-18.

Sourav K. B., Dibakar G., and Syamal K.D. (2011). Synchronization in counter-rotating oscillators, *CHAOS 21*, 033118(1-9).

Sprott J.C., (1994). Some simple chaotic flows. *Physical Review E*, **50(**2), 1-7.

Sundarapandian V., Aceng S., Sezgin K., and Unal, C. (2018). A New Finance Chaotic System, it's Electronic Circuit Realization, Passivity based Synchronization and an Application to Voice Encryption, *Nonlinear Engineering*, **8**(1), 293-205.

Yeldesbay, A., Jalan, S., & Dana, S. K. (2014). Chaos synchronization in coupled neurons with convection-diffusion interaction. *Nonlinear Dynamics*, **77**(1-2), 43-52.